Korean J. Chem. Eng., 35(4), 859-866 (2018)
DOI: 10.1007/s11814-017-0357-x

pISSN: 0256-1115
eISSN: 1975-7220

CO_2 gasification performance and alkali/alkaline earth metals catalytic mechanism of Zhundong coal char

Yun Liu, Yanjun Guan, and Kai Zhang†

Beijing Key Laboratory of Emission Surveillance and Control for Thermal Power Generation,
North China Electric Power University, Beijing 102206, China
(*Received 13 July 2017 • accepted 30 December 2017*)

Abstract−Gasification is generally considered as the most effective for low rank coal exploitation, and CO_2 gasification offers the advantage of upgrading a greenhouse gas. Herein, the effects of alkali and alkaline earth metals on gasification of char derived from Zhundong low rank coal (R-char) were investigated using a thermo-gravimetric analyzer (TGA). Additionally, the characteristics of chars were analyzed by X-ray fluorescence (XRF) and scanning electron microscopy (SEM) with energy dispersive spectroscopy (EDS). The results show that the carbon conversion increases as the temperature and CO_2 concentration increases. The R-char possesses a higher gasification rate and carbon conversion than the acid washing R-char (AR-char). It can be explained that the alkali and alkaline earth metals presence in coal char can remarkably facilitate the compound's decomposition and make more char surface exposure to react during the gasification process. For the kinetic analysis, the volumetric reaction model reveals a proper description among the three models (VRM, RPM, SCM), and the R-char and AR-char presents a compensation effect in VRM. Besides, the detailed correlation of two chars is $\ln(k_0)=0.10\ E_A-1.77$ (R-char) and $\ln(k_0)=0.10\ E_A-2.85$ (AR-char), respectively.

Keywords: Alkali and Alkaline Earth Metals, CO_2 Gasification, Compensation Effect, Catalytic, Zhundong Char

INTRODUCTION

The greenhouse effect due to CO_2 emissions has become a crucial issue in ecological self-purification and energy transformation [1,2]. However, the way of fossil fuel burning with CO_2 emissions still dominates today. Therefore, it is particularly important to research the gasification mechanism with CO_2, which can also create much more high value-added products and chemical functionality. As for the Zhundong coal, with an estimated reserve of 3.9 Gt, is a super large energy source in China [3]. It has a specific feature with high reactivity, medium volatile and low ash. Additionally, it also has high alkali and alkaline earth metals (AAEMs) in coal itself. Previous studies have indicated that the Zhundong coals can be utilized as CO_2 gasification [4-6], but accompanied by a relatively low gasification rate. As a result, the research about the CO_2 gasification performance and AAEMs catalytic mechanism of Zhundong coal chars has become a crucial problem.

To date, some studies about the correlation between AAEMs and the reactivity of CO_2 gasification have been investigated [7-10]. Dimple et al. [7] and Wu et al. [8] investigated the volatilization and catalytic effects of AAEMs on the pyrolysis and gasification of Victorian brown coal. It was stated that NaCl in the brown coal was mainly released as Na and Cl separately rather than as NaCl molecules, and the volatile-char interactions were affected by the valence of the AAEMs in the char. Meanwhile, several other studies focused on the transformation of Na, Cl and silica [7,11-13]. Kosminski et al. [12,13] indicated the transformation of Na during the gasification of South Australian lignite. Kosminski et al. [14] also investigated the reaction between Na and silica or kaolin, and found liquid sodium silicates were major reaction products of Na and silica. Ding et al. [9] further pointed out that the catalytic ability and concentration of AAEMs were positively correlated below a certain concentration. Moreover, Walker et al. [10] identified that catalytic ability of AAEMs on CO_2 gasification decreased in the order of Na>K>Ca from anthracite to lignite, and pointed out that the catalytic ability was dependent on the concentration, chemical forms and dispersion of AAEMs in coal. However, the fundamental mechanisms leading to the catalytic effect of AAEMs in Zhundong coal char have only had a scarce discussion.

Additionally, it is necessary to understand the reaction kinetics under controlled laboratory conditions to support large-scale gasification trials [5,15]. The common kinetic models, such as volumetric reaction model (VRM) [16], random pore model (RPM) [17] and the shrinking core model (SCM) [18] are widely proposed to predict Arrhenius parameters (E_A, k_0). The activation energy (E_A) and pre-exponential factor (k_0) are to evaluate reaction in kinetic analysis for coal gasification [19]. As one of the important methods to investigate the reaction kinetics of heterogeneous reactions [20], such as coal gasification [21], biomass pyrolysis [22], alkane hydrogenolysis [23], the compensation effect has been used to check the linear relationship between $\ln(k_0)$ and E_A in the Arrhenius equation. Therefore, it is important to investigate the compensation effect of Zhundong coal gasification with CO_2.

The objective of this study was to determine the CO_2 gasifica-

†To whom correspondence should be addressed.
E-mail: kzhang@ncepu.edu.cn

tion performance of chars derived from Zhundong coal, by considering the factors of reaction temperature and time, CO_2 concentration and AAEMs content. Furthermore, catalytic mechanism of AAEMs during char gasification and the compensation effect of Zhundong char were discussed.

MATERIAL AND METHODS

1. Char Preparation

Coal used in this study was from the east of the Junggar Basin in Xinjiang, China. Prior to experiment operation, all specimens were dried in a vacuum oven at 378 K for 2 h. To eliminate the effect of intra pore diffusion on the gasification rate, samples are ground and sieved with particle size less than 90 μm [16]. The proximate and ultimate analyses of Zhundong coal are summarized in Table 1.

Fig. 1 shows a schematic of a tubular reactor, which was primarily composed of intake part, sampling part and temperature control part. At the ignition stage of reaction, N_2 gas with the flow of 400 mL/min was used to replace the air within the reactor for 30 min. Then, the device was pre-heated to 1,073 K with a heating rate of 10 K/min. Coal samples were swiftly loaded into the reactor and maintained for 30 min under a continuous N_2 atmosphere. Char sample obtained was pushed to the cooling zone promptly by sample push rod and cooled to room temperature. The char sample named as R-char was taken out, a part of which was stored in a desiccator, while the other was washed with dilute sulfuric acid. Although the compositions of samples could be affected by acid washing method [24], 0.1 mol/L sulfuric acid was used to process the carbonaceous solid fuels to investigate the release and transformation of sodium [25], ignition temperature [24,26] and pyrolysis characteristics [27]. In this study, the R-char was stirred in 0.1 mol/L sulfuric acid for about 24 h under N_2 atmosphere. The solid to liquid ratio was 1 g solid sample to 30 mL solution. Then, the acid-washed char was washed with distilled water repeatedly until no indication of SO_4^{2-} in the solution by barium chloride and hydrochloric acid. Finally, the washed char was dried and referred to as AR-char.

Table 1. Proximate and ultimate analysis of Zhundong coal

Proximate analysis (wt%, a.d.)				Ultimate analysis (wt%, d.a.f.)				
V	FC	A	M	C	H	O[a]	N	S
28.15	59.25	3.08	9.52	70.79	3.86	24.26	0.56	0.53

[a]Oxygen was obtained by subtraction

2. Gasification Experiments

Gasification tests were carried out in the thermo-gravimetric analyzer (NETZSCH STA 449F3). The initial mass of sample is 10±0.3 mg, and all char samples are gasified isothermally at four different temperatures from 1,073 to 1,223 K. Under a continuous N_2 flow, the sample is placed at a crucible and heated at 30 K/min to the desired temperature. Then, the N_2 is replaced by CO_2 after the desired temperature is reached. The final temperature is kept for gasification until no weight loss changes. Three repeated runs for each sample are conducted to ensure the relative deviation is less than ±3%.

In this study, carbon conversion for gasification, X, is:

$$X = \frac{m_0 - m_t}{m_0 - m_{ash}} \quad (1)$$

where, m_0 is the initial mass of the sample, m_t is the mass at a particular time, and m_{ash} is the mass of the residual ash. Gasification rate is defined as differential of carbon conversion to gasification time, the gasification rate, r, is expressed as Eq. (2):

$$r = \frac{dX}{dt} \quad (2)$$

where, X is the carbon conversion, t refers to time.

3. Kinetic Models

Three common models for description of CO_2 gasification were adopted in this study. The first model is volumetric reaction model (VRM), which is an ideal model for describing gas-solid reaction. The reaction is considered to take place everywhere in the volume of the particle, as below:

$$\frac{dX}{dt} = k_{VRM}(1 - X) \quad (3)$$

where, k_{VRM} is the rate coefficient, t is time, X is the carbon conversion.

Or in the integrated form by Eq. (4):

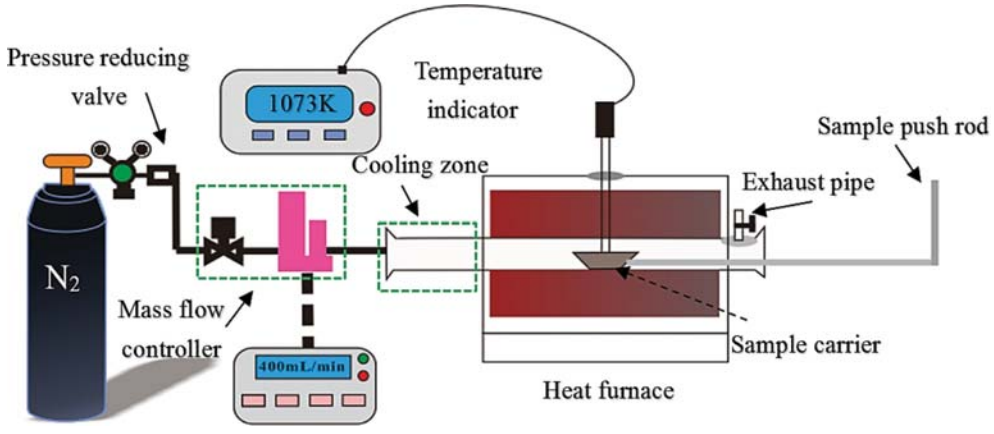

Fig. 1. Schematic diagram for the preparation of char samples.

$$\ln(1-X)=-k_{VRM}t \quad (4)$$

The second is the shrinking core model (SCM), which assumes that a porous particle consists of an assembly of uniform nonporous spherical grains and the reaction occurs at the surface of the samples. The model is given by:

$$\frac{dX}{dt}=k_{SCM}(1-X)^{2/3} \quad (5)$$

where, k_{SCM} is the rate coefficient, t is time, X is the carbon conversion.

Or in the integrated form by Eq. (6):

$$3[1-(1-X)^{1/3}]=k_{SCM}t \quad (6)$$

The random pore model (RPM) assumes that there is random overlapping of the pore surface during gasification.

$$\frac{dX}{dt}=k_{RPM}(1-X)\sqrt{1-\Psi\ln(1-X)} \quad (7)$$

where, k_{RPM} is the rate coefficient, t is time, X is the carbon conversion. Ψ is the structural parameter, which can be estimated according to relation [28]:

$$\Psi=\frac{2}{2\ln(1-X_{max})+1} \quad (8)$$

where, X_{max} is the carbon conversion when maximal reaction rate is observed.

The integrated form of Eq. (7) gives:

$$\frac{2}{\Psi}(\sqrt{1-\Psi\ln(1-X)}-1)=k_{RPM}t \quad (9)$$

Combining the well-known Arrhenius equation, the rate coefficient, k, can be expressed as:

$$k=k_0e^{-\frac{E_A}{RT}} \quad (10)$$

where, E_A is the activation energy, k_0 is the pre-exponential factor, R is the ideal gas law constant, and T is the temperature.

Taking logarithms of both sides of Eq. (10), it is written as:

$$\ln k=\ln k_0-\frac{E_A}{R}\frac{1}{T} \quad (11)$$

RESULTS AND DISCUSSION

1. Acid Washing Treatment

To investigate the effect of acid washing on R-char, the samples were ashed in a muffle furnace at 773 K according to the AS 1038.14.1-2003 (R2013) [5]. Briefly, approximately 0.5 g of each sample is thinly spread on a ceramic tray and then placed in the muffle furnace for 8 h. The ash sample is cooled to room temperature and collected. Table 2 lists the composition of the ash analyzed by X-ray fluorescence (Shimadzu XRF-1800). Here B/A is the ratio of basic oxides (CaO, MgO, Na_2O, Fe_2O_3, and K_2O) to acid oxides (SiO_2, Al_2O_3 and TiO_2). The B/A value of ash is 3.15, which means the R-char is dominated by basic oxides compared with acidic oxides. In contrast, the AR-char has a low B/A, which indicates the acid washing process can efficiently remove AAEMs.

The scanning electron microscopy coupled with energy dispersive X-ray spectroscopy (Tescan Vega 3) is used to characterize the morphology of the chars for obtaining semi-quantitative elemental analysis of the char particles. Figs. 2 and 3 show the SEM morphology and elements distribution map of R-char and AR-char, respectively. The average data of EDS value are summarized in Table 3. It can be found the AAEM elements (Ca, Mg, Na, K, Fe) in R-char are higher than those in AR-char, particularly in Na ele-

Table 2. Ash analysis of the char samples ashed at 773 K

Samples (wt%)	CaO	MgO	Na_2O	K_2O	Fe_2O_3	SiO_2	TiO_2	Al_2O_3	SO_3	Others
R-char	37.85	8.62	6.18	0.55	4.06	10.39	0.37	7.42	22.89	1.67
AR-char	7.34	1.15	0.61	0.68	1.71	48.98	0.92	27.54	9.88	1.19

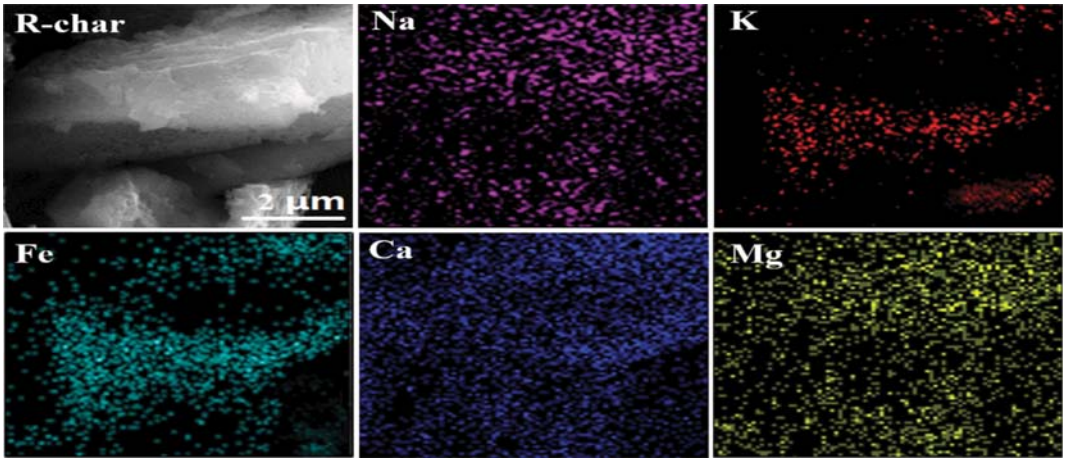

Fig. 2. SEM morphologies and element distribution map of R-char.

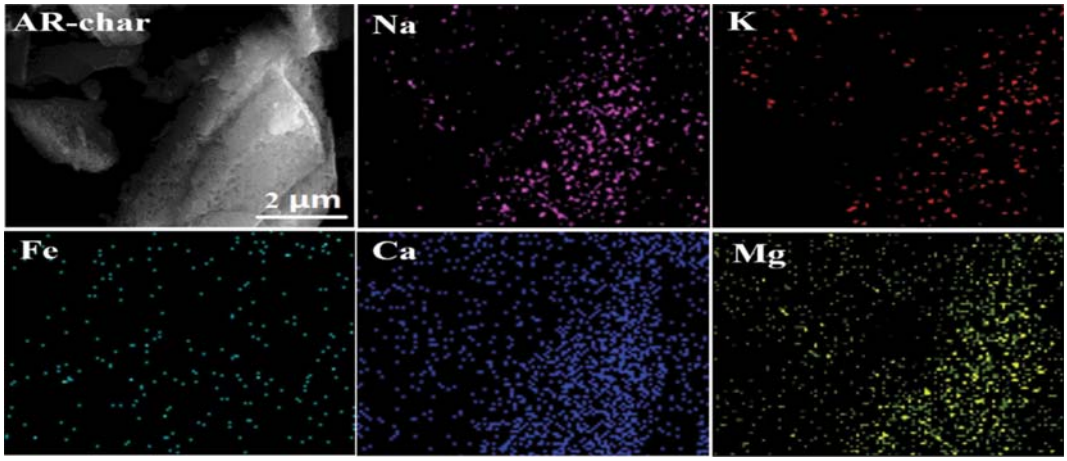

Fig. 3. SEM morphologies and elements distribution map of AR-char.

Table 3. EDS results of R-char and AR-char

Elements (wt%)	Ca	Mg	Na	K	Fe	Si	Al	Ti
R-char	32.58	12.37	9.42	1.69	8.76	19.21	15.36	0.61
AR-char	16.07	6.86	4.94	0.68	1.83	39.65	29.12	0.85

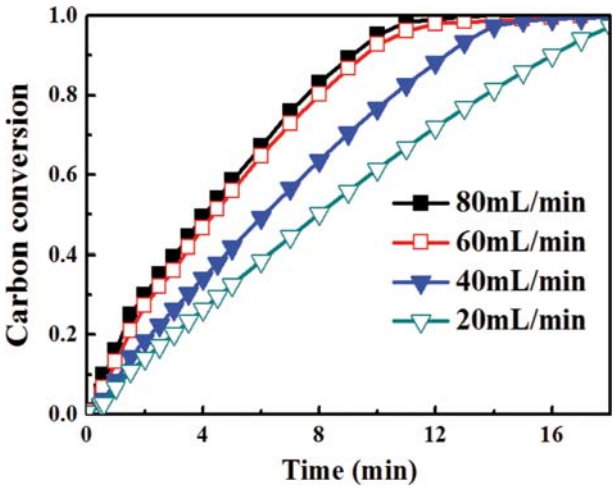

Fig. 4. Effect of CO_2 flow on carbon conversion for R-char.

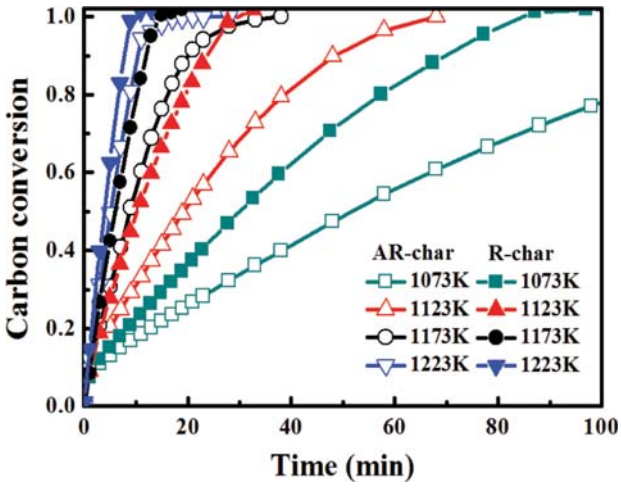

Fig. 5. Effect of temperature on carbon conversion for AR-char and R-char (80% CO_2).

ment, which proves that the acid washing method can effectively remove the majority of AAEMs from R-char. The above finding is also consistent with chemical composition of two chars in Table 2.

2. Effect of External Diffusion on Gasification

The increasing flow of reactant gas can largely neglect the external diffusion to some extent, which is a common way for certain amounts of sample gasification [29]. Fig. 4 shows the effect of CO_2 flows on R-char gasification at 1,173 K. The results indicate the carbon conversion increases significantly with an increase in CO_2 flow when it is less than 60 mL/min. However, the conversion hardly changes when the flow is more than 60 mL/min. Consequently, the CO_2 flow of the sample is fixed at 80 mL/min in the following experiments. Combined with section 2.1, the effect of diffusion can be ignored when the particle size is less than 90 μm under the flow of 80 mL/min.

3. Effect of Temperature on Gasification

The processed conversion results for samples are presented in Fig. 5. The carbon conversion of both samples increases as temperature increases from 1,073 K to 1,223 K. The carbon conversion of R-char is higher than that of AR-char under the same conditions, especially in the low temperature regions, which is mainly attributed to the presence of AAEMs in char itself. However, the difference in carbon conversion of two chars is gradually decreased as the temperature increased. According to molecular collision theory [30], changes in the number of reactive collisions are taking place during the reaction, and the number of active sites is also changed. The more active the sites are, the easier gasification reactions happen. It is well known that the number of reactive colli-

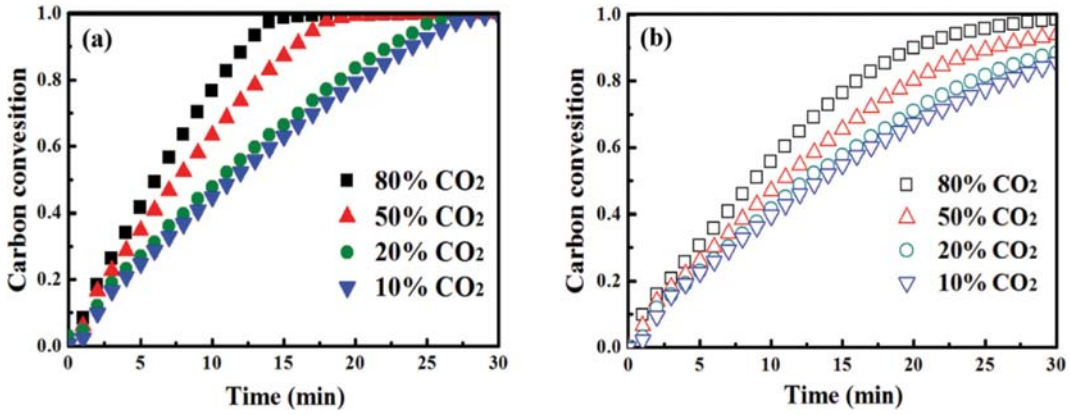

Fig. 6. Effect of CO_2 concentration on carbon conversion for R-char (a) and AR-char (b) at 1,173 K.

sions increases as the temperature increased. As a result, it can be obtained that carbon conversion rises at high temperatures.

4. Effect of CO_2 Concentration on Gasification

Fig. 6 shows the carbon conversion of R-char and AR-char gasification at 1,173 K with various CO_2 concentrations. In accordance with the kinetics theory of coal gasification, the carbon conversion increased as the concentration of CO_2 increased in the whole process. Thus, the reaction time of two chars with a fixed carbon conversion is reduced as the concentration of CO_2 ranges from 10% (v/v) to 80% (v/v), whereas a not obvious result is achieved when the CO_2 concentration is between 10% (v/v) and 20% (v/v). In addition, the carbon conversion of R-char is higher than that of the AR-char at the corresponding time (Fig. 6(a), (b)), which is mainly due to the more AAEMs presence in R-char, as listed in Table 2 and 3. Consistent results were obtained in Argentinean subbituminous chars [31].

5. Effect of AAEMs on Gasification

R-char and AR-char were gasified with CO_2 to study the roles of the AAEMs on gasification reaction. As shown in Fig. 7, the gasification rate initially increases and then decreases, in which the maximum value of carbon conversion is obtained at around 0.07.

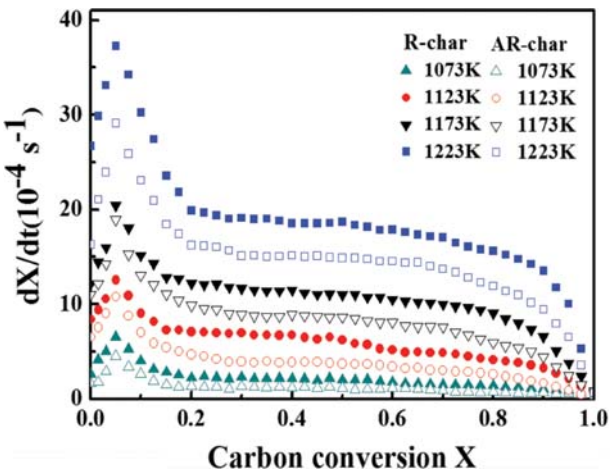

Fig. 7. Gasification rate vs carbon conversion for R-char and AR-char (80% CO_2).

The main reason is the changes of active surface sites and activation energy during the coal gasification process [32]. Combining the B/A values of ash from R-char (3.15) and AR-char (0.15) in Table 2 and Figs. 2 and 3, the reactivity reduction is mainly due to decreasing active sites after AAEMs removal. The above findings further revealed that the AAEMs play an important catalytic role in coal gasification reaction.

Carbon-oxygen complexes in the formation of coal gasification are closely associated with the reactivity, and the essence of gasification process is the decomposition of carbon-oxygen complexes, which can be expressed as follows:

$$C_f+CO_2 \rightarrow C_f(0)+CO \quad (12)$$

$$C_f(0) \rightarrow CO+C_f \quad (13)$$

where, C_f is the carbon atom at the edge of the coal surface, $C_f(O)$ is the carbon-oxygen complex in the formation of gasification process.

The AAEMs have two main forms present in high sodium coal, as carboxylates and as soluble salts (mainly -COONa and NaCl) [33]. The Na existing as NaCl behaves differently from that as sodium carboxylates (-COONa) during pyrolysis [34]. NaCl in char is not a very active catalyst [35], while it may have catalytic effects on the char reactivity as a result of transformations of NaCl during the devolatilization. It has been proved that the sodium carboxylate is less volatile than NaCl during pyrolysis. Based on the kinetic simulation, Van Eyk et al. [36] found that approximately 33% NaCl was released, but only a little sodium carboxylate during devolatilization of a similar coal. Apart from NaCl released into the gas phase, some catalytic effects of NaCl are likely to react with the carboxylic acid groups within the coal structure, thus retaining Na and releasing HCl, which can be expressed as follows [36,37]:

$$-(COOH)+NaCl \rightarrow -(COONa)+HCl \quad (14)$$

For the sodium existing as sodium carboxylates (-COONa), a major proportion of sodium is bonded to oxygen in the char matrix to form O^-Na^+ bond. What is more, sodium bonded to oxygen in the char matrix participates in the metal-carbon bond formations, which results in migration of the surface charge. It could change electron-cloud distribution of the surface carbon

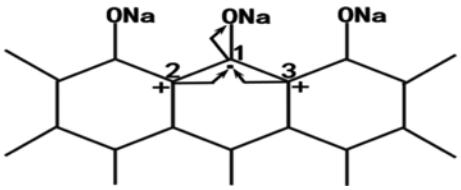

Fig. 8. Schematic diagram for alkali metal combined with carbon on the edge of char surface.

atoms, which is also beneficial for chars to participate in the reaction. As shown in Fig. 8, the electron-cloud of carbon atom, 1, moves to the strong electron-withdrawing group, O^-Na^+, which makes the adjacent carbon atoms, 2 and 3, partially lose electrons. Therefore, the carbon atoms, 2 and 3, are given electronegativity. The positively charged carbon is easier to combine with the negatively charged oxygen. Therefore, alkali metals are advantageous to the gasification reaction.

In the catalytic reaction, the catalysis of alkaline earth metals, such as Ca and Fe, is described with redox cycle reaction [38]. These reactions are as follows:

$$MO+C_f \rightarrow C_f(0)+M \quad (15)$$

$$M+CO_2 \rightarrow MO+CO \quad (16)$$

$$(0) \rightarrow CO+C_f \quad (17)$$

where, MO is the oxidation of alkaline earth metal, M is the reduction of alkaline earth metal, C_f is the carbon atom on the edge of the coal surface, C_f (O) refers to the carbon-oxygen complex. Generally, the alkali and alkaline earth metals presence in coal char can accelerate complexes decomposition and expose more char surface to react during the gasification process.

6. Kinetic Analysis

To evaluate the applicability of selected kinetic models, Eqs. (4), (6) and (9) are used to predict the conversion over time and compared with the experimental data. As shown in Fig. 9, the volumetric reaction model (VRM) gives a reasonable description about the carbon conversion in temperature region of 1,073 K to 1,123 K, especially at the lower temperatures (1,073 K, 1,123 K). This finding is consistent with the results from the non-catalytic steam gasification of lignite char [39]. Therefore, VRM is a proper analysis method on kinetic of char gasification.

Substituting Eq. (4) into Eq. (11), it is given by:

$$\ln\left[-\frac{\ln(1-X)}{t}\right]=\ln k_0-\frac{E_A}{R}\frac{1}{T} \quad (18)$$

The Arrhenius parameters (E_A, k_0) are calculated by Eq. (18) based on experimental data.

E_A is the least energy required for a reaction in the gasification process. The k_0 is a collective constant accounting for the crowd of rate-influencing parameters, such as molecular orientation, gaseous reactant concentration, active sites and so on. Table 4 lists the kinetic parameters (E_A, k_0) of samples at different carbon conversions. The calculated values indicate that, as the gasification reaction proceeds, the values of E_A increased (or decreased) accompanied by a simultaneous increase (or decrease) of the k_0 value. The result

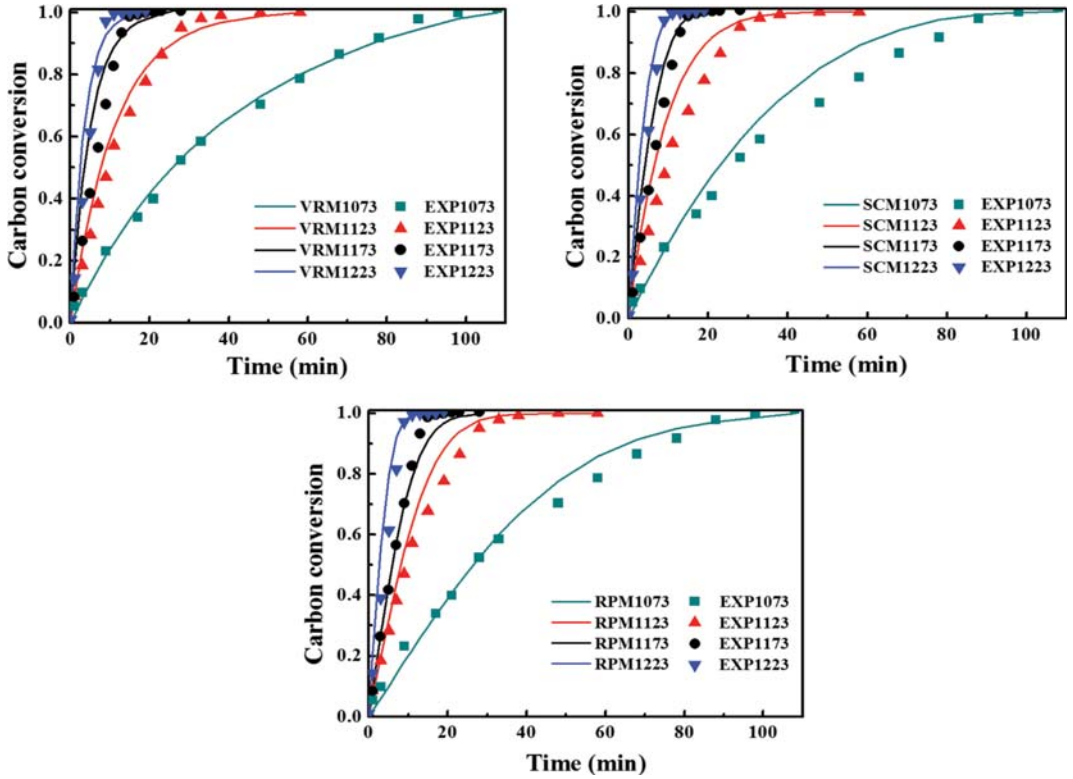

Fig. 9. Plots fitting the VRM, the SCM and the RPM to the experimental data for gasification of R-char at temperatures of 1,073, 1,123, 1,173 and 1,223 K.

Table 4. Arrhenius parameters (E_A, k_0) for R-char and AR-char

X	E_A, (kJ/mol)		k_0, (1/min)	
	R-char	AR-char	R-char	AR-char
0.2	139.34	145.66	1.72×10^5	2.05×10^5
0.3	145.15	152.66	2.97×10^5	6.55×10^5
0.4	147.45	174.12	3.79×10^5	4.37×10^6
0.5	152.65	181.10	6.88×10^5	1.06×10^7
0.6	150.81	177.84	5.93×10^5	6.90×10^6
0.7	147.57	169.89	4.54×10^5	2.67×10^6
0.8	141.33	165.12	2.56×10^5	1.57×10^6

suggests that the "compensation effect" is presented in the reaction. Some rise of the E_A is accompanied with a simultaneous increase of k_0 for carbon conversion from 0.2 to 0.5, while some decrease of E_A is compensated by decrease of k_0 after conversion is 0.5. It can be due to the relaxed aromatic structure of char, more stable carbon atom involving gasification, which requires the cleaving of increasingly stronger bonds. Therefore, the reactants should overcome a higher energy barrier, resulting in an increased activation energy. With prolonged reaction time, the char structures were gradually disintegrated. Since the carbonaceous material was already consumed, the activation energy was decreased. It is also found that the R-char has considerably lower activation energy than that of AR-char.

Fig. 10 quantitatively illustrates the compensation effect for R-char and AR-char conversion from 0.2 to 0.8 (references selected by most of the works in kinetics literatures [40,41]). A linear interrelationship with good approximation is observed for both samples. The gradient is the ratio of $\ln k_0$ and E_A in the kinetic compensation effect, so it can be used as an indication of the nature of the carbon structural condensation evolution. Furthermore, the initial carbon structure controls the intercept. In the presence of catalytic effect (for the R-char), a different intercept value is obtained in comparison with the acid-washed char, and the extent of evolution of activation energy is different from the AR-char. However, the gradient value for R-char is similar to AR-char (approximately 0.10). These suggest that the AAEMs may alter the reaction pathway during the gasification process [42].

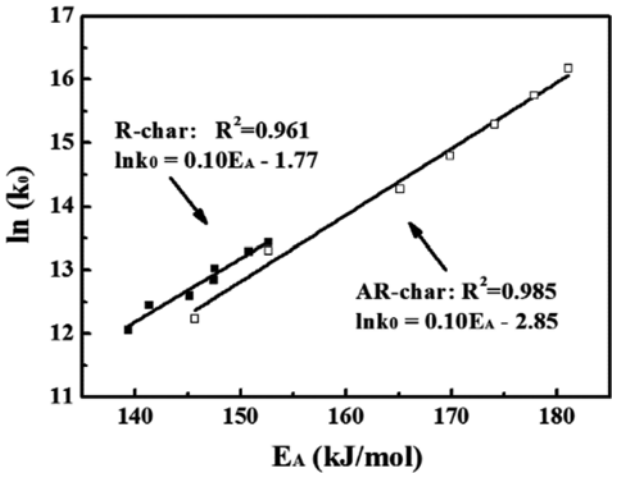

Fig. 10. Compensation effect of R-char and AR-char in isothermal CO_2 gasification.

CONCLUSIONS

The CO_2 gasification reactivity of chars derived from Zhundong coal was determined by thermo-gravimetric analysis. The following conclusions are obtained from this work:

(1) Acid washing can remove the majority of AAEMs from R-char. External diffusion can be neglected when the flow of reactant gas is 80 mL/min in the range of this study.

(2) Carbon conversion increases as the temperature and CO_2 concentration increase. The reactivity of AR-char is much lower than that of R-char. It demonstrates that AAEMs can accelerate compound's decomposition and expose more char surface to react during the gasification process.

(3) For the kinetic analysis, the volumetric reaction model gives a proper description, and R-char and AR-char both present a compensation effect. The detailed correlation of two chars is $\ln(k_0)=0.10\,E_A-1.77$ (R-char) and $\ln(k_0)=0.10\,E_A-2.85$ (AR-char), respectively. Moreover, the AAEMs may alter the reaction pathway during gasification.

ACKNOWLEDGEMENTS

Authors gratefully acknowledge National Natural Science Foundation of China (U1610254, 91434120), Major Special Project of Shanxi Province (MD2014-03, MD2015-01) and Fundamental Research Funds for the Central Universities (2017XS051).

ABBREVIATIONS

The following abbreviations are used in this manuscript:

AAEMs : alkali and alkaline earth metals
TGA : thermo-gravimetric analyzer
VRM : volumetric reaction model
SCM : shrinking core model
RPM : random pore model
E_A : activation energy
SEM : scanning electron microscopy
EDS : energy dispersive X-ray spectroscopy
R^2 : coefficient of determination

REFERENCES

1. S. J. Wang, C. L. Fang, X. L. Guan, B. Pang and H. T. Ma, *Appl. Energy*, **136**, 738 (2014).
2. B. T. Zhao, W. W. Tao, M. Zhong, Y. X. Su and G. M. Cui, *Renew Sust. Energy Rev.*, **65**, 44 (2016).
3. J. B. Li, M. M. Zhu, Z. Z. Zhang, K. Zhang, G. Q. Shen and D. K. Zhang, *Fuel Process. Technol.*, **149**, 176 (2016).
4. M. M. Wang, J. S. Zhang, S. Y. Zhang, J. H. Wu and G. X. Yue, *Korean J. Chem. Eng.*, **25**(6), 1322 (2008).
5. T. Joanne and B. Sankar, *Chem. Eng. J.*, **285**, 331 (2016).
6. T. J. Kang, H. J. Park, H. Namkung, L. H. Xu, S. M. Fan and H. T.

Kim, *Korean J. Chem. Eng.*, **34**(4), 1238 (2017).
7. M. Q. Dimple, H. W. Wu and C. Z. Li, *Fuel*, **81**, 143 (2002).
8. H. W. Wu, M. Q. Dimple and C. Z. Li, *Fuel*, **81**, 1033 (2002).
9. L. Z. Ding, J. Zhou and Q. H. Guo, *Fuel*, **142**, 134 (2015).
10. P. L. Walker, S. Matsumoto and T. Hanzawa, *Fuel*, **62**, 140 (1983).
11. Y. H. Bai, S. H. Zhu, K. Luo, M. Q. Gao, L. J. Yan and F. Li, *Appl. Therm. Eng.*, **112**, 156 (2017).
12. A. Kosminski, D. P. Ross and J. B. Agnew, *Fuel Process. Technol.*, **87**, 943 (2006).
13. A. Kosminski, D. P. Ross and J. B. Agnew, *Fuel Process. Technol.*, **87**, 1037 (2006).
14. A. Kosminski, D. P. Ross and J. B. Agnew, *Fuel Process. Technol.*, **87**, 1051 (2006).
15. H. Y. Park and D. H. Ahn, *Korean J. Chem. Eng.*, **24**(1), 24 (2007).
16. R. Silbermann, A. Gomez, I. Gates and N. Mahinpey, *Ind Eng Chem Res.*, **52**, 14787 (2013).
17. J. W. Kook, I. S. Gwak, Y. R. Gwak, M. W. Seo and S. H. Lee, *Korean J. Chem. Eng.*, **34**(12), 3092 (2017).
18. S. Sawettaporn, K. Bunyakiat and B. Kitiyanan, *Korean J. Chem. Eng.*, **26**(4), 1009 (2009).
19. M. Nader and G. Arturo, *Chem. Eng. Sci.*, **148**, 14 (2016).
20. L. Liu and Q. X. Guo, *Chem. Rev.*, **101**, 673 (2001).
21. H. W. Wu, X. J. Li, J. J. Hayashi, T. Chiba and C. Z. Li, *Fuel*, **84**, 1221 (2005).
22. E. L. K. Mui, W. H. Cheung, V. K. C. Lee and G. McKay, *Waste Manage.*, **30**, 821 (2010).
23. G. C. Bond, *Appl. Catal. A: Gen.*, **191**, 23 (2000).
24. L. Wu, Y. Qiao, B. Gui, C. Wang, J. Y. Xu, H. Yao and M. H. Xu, *Energy Fuel*, **26**, 112 (2012).
25. S. Liu, Y. Qiao, Z. L. Lu, B. Gui, M. M. Wei, Y. Yu and M. H. Xu, *Energy Fuel*, **28**, 1911 (2014).
26. Y. Qiao, L. Zhang, E. Binner, M. H. Xu and C. Z. Li, *Fuel*, **89**, 3381 (2010).
27. C. Sathe, Y. Y. Pang and C. Z. Li, *Energy Fuel*, **13**, 748 (1999).
28. J. Ochoa, M. C. Cassanello, P. R. Bonelli and A. L. Cukierman, *Fuel Process. Technol.*, **74**, 161 (2001).
29. W. Huo, Z. J. Zhou, F. C. Wang, Y. F. Wang and G. S. Yu, *Fuel*, **131**, 59 (2014).
30. G. Skodras, G. Nenes and N. Zafeiriou, *Appl. Therm. Eng.*, **74**, 111 (2015).
31. G. D. Micco, A. Nasjleti and A. E. Bohe, *Fuel*, **95**, 537 (2012).
32. A. N. Rollinson and M. K. Karmakar, *Chem. Eng. Sci.*, **128**, 82 (2015).
33. D. M. Quyn, H. Wu, J. I. Hayashi and C. Z. Li, *Fuel*, **82**, 587 (2003).
34. D. M. Quyn, H. W. Wu, S. P. Bhattacharya and C. Z. Li, *Fuel*, **81**, 151 (2002).
35. R. J. Lang. *Fuel*, **65**, 1324 (1986).
36. P. J. vanEyk, P. J. Ashman, Z. T. Alwahabi and G. J. Nathan, *Combust. Flame*, **158**(6), 1181 (2011).
37. A. Kosminski, D. P. Ross and J. B. Agnew, *Fuel Process. Technol.*, **87**(11), 943 (2006).
38. A. H. Clemens, L. F. Damiano and T. W. Matheson, *Fuel*, **77**, 1017 (1988).
39. T. W. Kwon, J. R. Kim, S. D. Kim and W. H. Park, *Fuel*, **68**, 416 (1989).
40. G. Aranda, A. J. Grootjes, C. M. Meijden, A. Drift, D. F. Gupta, R. R. Sonde, S. Poojari and C. B. Mitra, *Fuel Process. Technol.*, **141**, 16 (2016).
41. C. D. Blasi, *Prog. Energy Combust. Sci.*, **35**, 121 (2009).
42. K. Yip, E. Ng, C. Z. Li, J. I. Hayashi and H. W. Wu, *P. Combust. Inst.*, **33**, 1755 (2011).